

Title: Relativistic Dynamics of Graphene

Date: Apr 16, 2008 02:00 PM

URL: <http://pirsa.org/08040014>

Abstract: Graphene, a single atomic layer of graphite, was created only a few years ago. It is a remarkable system, whose low energy effective theory has a lot in common with relativistic 2 + 1 dimensional ones. Graphene allows tabletop experiments for observing nonperturbative relativistic phenomena, most notably spontaneous chiral symmetry breaking both in vacuum and in an external magnetic field. The latter is in turn crucial for the dynamics of Quantum Hall effect in this system. I will review the basic physics and the latest results obtained both in the experimental studies and the theory of graphene.

*Relativistic Dynamics
in Graphene*

Graphene — a one-atom-thick layer of graphite (crystalline carbon).

K. Novoselov, A. Geim et al., *Science*,
306 (2004) 666

Method to produce: repeated peeling of a piece of graphite with Scotch tape

Relativistic like brane world dynamics:

electrons live on a plane;
electromagnetic field is in 3 dim. bulk

Dispersion relation for quasiparticles:

$$\omega \approx v_F |\vec{k}| ; \quad v_F \approx 10^6 \text{ m/s} ;$$

$$v_F/c \approx 1/300$$

P. Wallace, 1947)

Graphene — a one-atom-thick layer of graphite (crystalline carbon).

K. Novoselov, A. Geim et al., *Science*,
306 (2004) 666

Method to produce: repeated peeling of a piece of graphite with Scotch tape

Relativistic like brane world dynamics:

electrons live on a plane;
electromagnetic field is in 3 dim. bulk

Dispersion relation for quasiparticles:

$$\omega \approx v_F |\vec{k}| ; \quad v_F \approx 10^6 \text{ m/s} ;$$

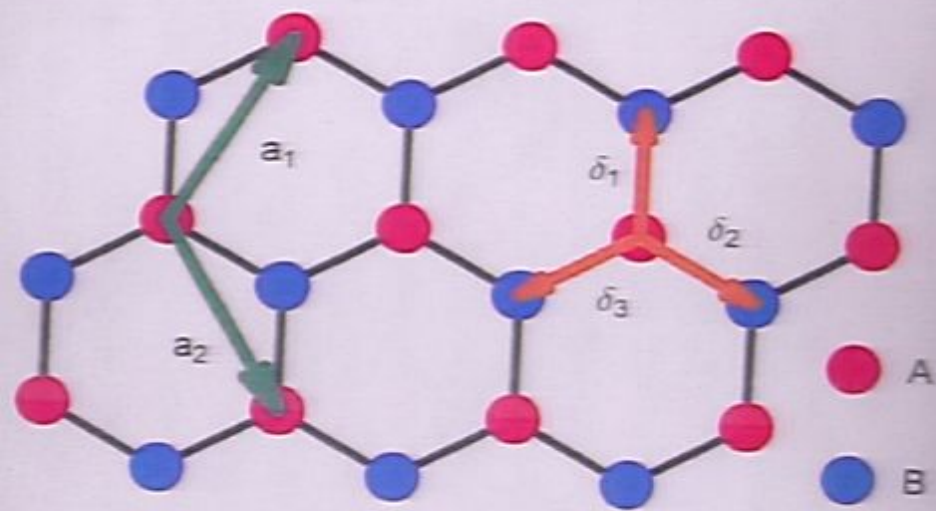
$$(P. Wallace, 1947) \quad v_F/c \approx 1/300$$



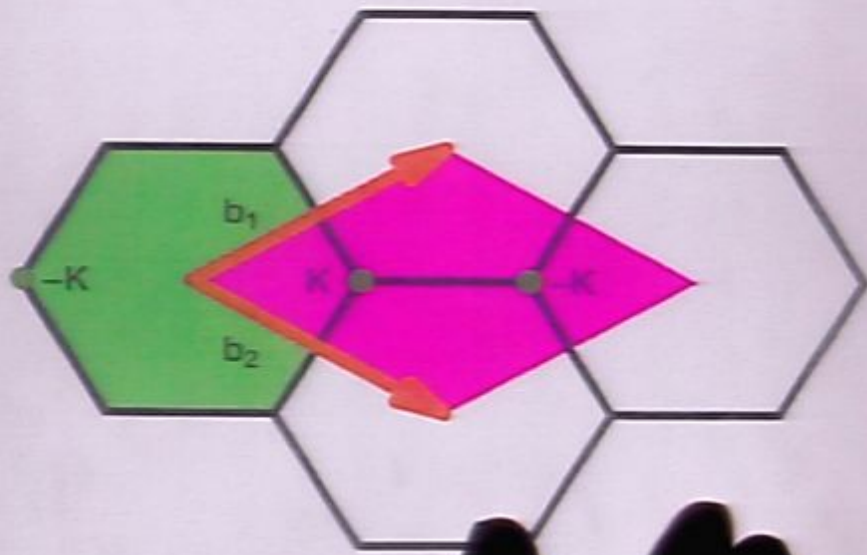
Figure 2. Characterization of single crystals: the thinnest material you will ever see. (a) Graphene (isolated by successive micromechanical exfoliation) on copper foil. The white region indicating a relative length of $\sim 4\ \mu\text{m}$ clearly indicates that it is a single layer. (b) A graphene sheet freshly exfoliated on a microscopic metallic substrate. The transmission electron microscopy image is adapted from ref. 18. (c) Raman spectroscopy micrograph of a relatively large graphene crystal, which shows that most of the crystal's faces are single and structure edges are indicated by the colored lines and observed in the main ^{13}C Raman. K.S.N., P. Ballew et al. (KUC) (reproduced). (D) Raman along stripe edges and longitudinal direction are essential to detect significant structure.

Graphene's quality clearly reveals itself in a pronounced ambipolar electric field effect (Fig. 3a) such that charge carriers can be tuned continuously between electrons and holes in concentrations n as high as $10^{12}\ \text{cm}^{-2}$ and their mobilities μ can exceed $15,000\ \text{cm}^2/\text{Vs}$ even under ambient conditions.¹⁹ Moreover, the observed mobilities weakly depend on temperature T , which means that μ at 300K is still limited by impurity scattering and, therefore, can be improved significantly, perhaps, even up to $\sim 100,000\ \text{cm}^2/\text{Vs}$. Although some semiconductors exhibit room-temperature μ as high as $\sim 10^5\ \text{cm}^2/\text{Vs}$ (mainly, holes), these values are quoted for undoped bulk semiconductors. In graphene, μ remains high even at high n ($\sim 10^{12}\ \text{cm}^{-2}$) in both electrochemically doped devices²⁰ while maintaining low ballistic transport on submicron scale (up to $\sim 2\ \mu\text{m}$) at 300K.²¹ A further indication of the system's extreme electronic quality is the quantum Hall effect (QHE) that can be observed in graphene even at room temperature (Fig. 3b), extending the previous temperature range for the QHE by a factor of 10.

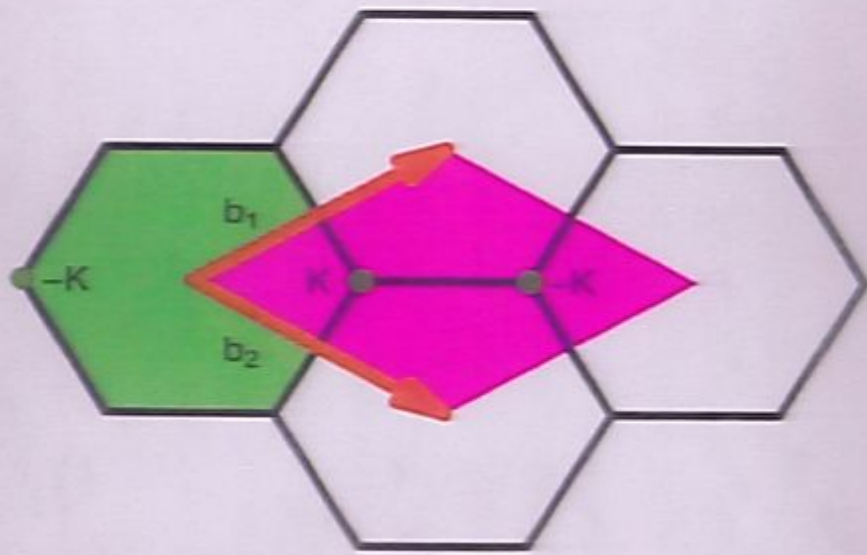
An equally important reason for the success of graphene is a unique nature of its charge carriers. In condensed matter physics, the Schrödinger equation rules the world, usually being quite sufficient to describe electronic properties of materials. Graphene is an exception: its charge carriers move relativistic particles and are more and more natural to describe starting with the Dirac equation rather than the Schrödinger equation.^{22,23} Although there is nothing particularly mysterious about particles moving around carbon atoms, their movement



(b)



(b)



Dirac Equation in Graphene

G. Semenoff, PRL, 53 (1984) 2449

$$[i\hbar\gamma^0\partial_t + i\hbar v_F\gamma^1\partial_x + i\hbar v_F\gamma^2\partial_y]\psi_s(t, \vec{r}) = 0,$$

$s = \pm$ is the spin index playing here the role of flavor;

$$\psi_s = (\psi_{KA}, \psi_{KB}, \psi_{K'B}, \psi_{K'A})_s$$

$$\gamma^\mu = (\gamma^0, \gamma^1, \gamma^2) = \tilde{T}_{KK'}^3 \otimes (\tilde{T}^3, i\tilde{T}^2, -i\tilde{T}^1)_{AB}$$

Lorentz symmetry in 2+1 dimensions, with v_F playing the role of light velocity

Extended chiral symmetry:

$$\{\gamma^3, \gamma^\nu\} = 0, \quad \{\gamma^5, \gamma^\nu\} = 0; \quad \nu = 0, 1, 2$$

$U(4)$ symmetry with 16 generators:

$$\frac{\sigma^a}{2} \otimes I_4, \quad \frac{\sigma^a}{2i} \otimes \gamma^3, \quad \frac{\sigma^a}{2} \otimes \gamma^5, \quad \frac{\sigma^a}{2} \otimes \gamma^3 \gamma^5,$$

where I_4 - 4x4 Dirac unit matrix,

$$\gamma^3 = i \begin{pmatrix} 0 & I \\ I & 0 \end{pmatrix}, \quad \gamma^5 = i \begin{pmatrix} 0 & I \\ -I & 0 \end{pmatrix}, \quad \gamma^3 \gamma^5 = \begin{pmatrix} I & 0 \\ 0 & -I \end{pmatrix}$$

σ^a - four Pauli matrices acting on spin
(σ^0 - 2x2 unit matrix).

Extended chiral symmetry:

$$\{\gamma^\mu, \gamma^\nu\} = 0, \quad \{\gamma^5, \gamma^\nu\} = 0; \quad \nu = 0, 1, 2$$

$U(4)$ symmetry with 16 generators:

$$\frac{\sigma^a}{2} \otimes I_4, \quad \frac{\sigma^a}{2i} \otimes \gamma^3, \quad \frac{\sigma^a}{2} \otimes \gamma^5, \quad \frac{\sigma^a}{2} \otimes \gamma^3 \gamma^5,$$

where I_4 - 4×4 Dirac unit matrix,

$$\gamma^3 = i \begin{pmatrix} 0 & I \\ I & 0 \end{pmatrix}, \quad \gamma^5 = i \begin{pmatrix} 0 & I \\ -I & 0 \end{pmatrix}, \quad \gamma^3 \gamma^5 = \begin{pmatrix} I & 0 \\ 0 & -I \end{pmatrix}$$

σ^a - four Pauli matrices acting on spin
(σ^0 - 2×2 unit matrix).

Extended chiral symmetry:

$$\{\gamma^3, \gamma^\nu\} = 0, \quad \{\gamma^5, \gamma^\nu\} = 0; \quad \nu = 0, 1, 2$$

$U(4)$ symmetry with 16 generators:

$$\frac{\sigma^a}{2} \otimes I_4, \quad \frac{\sigma^a}{2i} \otimes \gamma^3, \quad \frac{\sigma^a}{2} \otimes \gamma^5, \quad \frac{\sigma^a}{2} \otimes \gamma^3 \gamma^5,$$

where I_4 - 4x4 Dirac unit matrix,

$$\gamma^3 = i \begin{pmatrix} 0 & I \\ I & 0 \end{pmatrix}, \quad \gamma^5 = i \begin{pmatrix} 0 & I \\ -I & 0 \end{pmatrix}, \quad \gamma^3 \gamma^5 = \begin{pmatrix} I & 0 \\ 0 & -I \end{pmatrix}$$

σ^a - four Pauli matrices acting on spin
(σ^0 - 2x2 unit matrix).

Adding Dirac mass term

$$\tilde{\Delta} \bar{\psi} \psi \equiv \tilde{\Delta} \psi^\dagger \gamma^0 \psi, \quad \tilde{\Delta} \equiv m^2 v_F^2,$$

would break the $U(4)$ down to $U(2)_a \times U(2)_b$ with generators

$$\underline{\frac{\tilde{G}^a}{2} \otimes I_4}, \quad \underline{\frac{\tilde{G}^a}{2} \otimes \gamma^3 \gamma^5}$$

chiral (excitonic) condensate:

$$\langle \bar{\psi} \psi \rangle = n_{KA} + n_{K'A} - n_{KB} - n_{K'B},$$

$n_{KA} = \langle \psi_{KA}^\dagger \psi_{KA} \rangle$, etc — electron densities at specified valleys, K and K' , and sublattices, A and B .

$\langle \bar{\psi} \psi \rangle \neq 0 \implies$ density imbalance between A and B sublattices (charge density wave).

Adding Dirac mass term

$\tilde{\Delta} \bar{\psi} \psi \equiv \tilde{\Delta} \psi^\dagger \gamma_0 \psi$, $\tilde{\Delta} \equiv m^2 v_F^2$,
would break the $U(4)$ down
to $U(2)_a \times U(2)_b$ with generators
 $\frac{G^d}{2} \otimes I_4$, $\frac{G^d}{2} \otimes \gamma^3 \gamma^5$

chiral (excitonic) condensate:

$$\langle \bar{\psi} \psi \rangle = n_{KA} + n_{K'A} - n_{KB} - n_{K'B},$$

$n_{KA} = \langle \psi_{KA}^\dagger \psi_{KA} \rangle$, etc — electron densities at specified valleys, K and K' , and sublattices, A and B .

$\langle \bar{\psi} \psi \rangle \neq 0 \implies$ density imbalance between A and B sublattices (charge density wave).

Could a Dirac mass be generated dynamically?

More about dynamics in graphene

Because $v_F \neq c$, including electromagnetic interactions leads to Lorentz symmetry breaking. In particular, because $v_F/c \approx \frac{1}{300} \ll 1$, static Coulomb interactions dominate. However, scale (dilation) symmetry is still (classically) exact.

Could a Dirac mass be generated dynamically?

More about dynamics in graphene

Because $v_F \neq c$, including electromagnetic interactions leads to Lorentz symmetry breaking. In particular, because $v_F/c \approx \frac{1}{300} \ll 1$, static Coulomb interactions dominate. However, scale (dilation) symmetry is still (classically) exact.

Effective coupling constant

$$g \equiv \frac{e^2}{\hbar v_F \epsilon} = \frac{c}{v_F \epsilon} \frac{e^2}{\hbar c} =$$
$$\approx \frac{c}{v_F \epsilon} \frac{1}{137} \approx \frac{300}{\epsilon 137} \sim 1 \text{ for } \epsilon \sim 2-4.$$

Theoretical analysis:

E. Gorbar, V. Gusynin, V. M., and
I. Shovkova, Phys. Rev. B. 66 (2002) 045108

$$g_{cr} \approx 2.3$$

D. Khveshchenko and H. Lee, Nucl. Phys.
B 687 (2004) 323

$$g_{cr} \approx 1.1$$

Experiment: there is no gap
in graphene.

fine structure constant

$$g \equiv \frac{e^2}{\hbar v_F \epsilon} = \frac{c}{v_F \epsilon} \frac{e^2}{\hbar c} =$$
$$\approx \frac{c}{v_F \epsilon} \frac{1}{137} \approx \frac{300}{\epsilon 137} \sim 1 \text{ for } \epsilon \sim 2-4.$$

Theoretical analysis:

E. Gorbar, V. Gusynin, V. M., and
I. Shovkova, Phys. Rev. B. 66 (2002) 045108

$$g_{cr} \approx 2.3$$

D. Khveshchenko and H. Lee, Nucl. Phys.
B 687 (2004) 323

$$g_{cr} \approx 1.1$$

Experiment: there is no gap
in graphene.

of $\epsilon \sim 2-4$ for $\epsilon \sim 2-4$.
E137

Theoretical analysis:

E. Gorbar, V. Gusynin, V. M., and
I. Shorikov, Phys. Rev. B. 66 (2002) 045108

$$g_{cr} \approx 2.3$$

D. Khveshchenko and H. Lead, Nucl. Phys.
B 687 (2004) 323

$$g_{cr} \approx 1.1$$

Experiment: there is no gap
in graphene.

But it is not the end of the story: In the rest of this talk, I will argue (show?) that a Dirac mass, actually two different types of Dirac masses, have been already observed in graphene in a strong magnetic field.

Magnetic catalysis phenomenon

A constant magnetic field is a strong catalyst of dynamical chiral symmetry breaking, leading to the generation of a fermion dynamical mass even at the weakest attractive interaction between fermions.

V. Gusynin, V. M., and I. Shovkova,
Phys. Rev. Lett. 73, 3499 (1994);

Nucl. Phys. B 462, 249 (1996)

$D=3+1$ and $D=2+1$ cases.

Extension to $D=d+1$, $d \geq 3$ in

E. Gorbar, Phys. Lett. B 491, 305 (2000)

The LLL fermion propagator:

$$S(x, y) = \exp\left[\frac{ieB}{2} \epsilon^{ab} x^a y^b\right] \cdot \tilde{S}(x-y); \quad a, b = 1, 2$$

Schwinger phase

$$\tilde{S}(K) = 2i e^{\frac{-K_1^2}{ieB}} \frac{K^0 \gamma^0 - K^3 \gamma^3 + m}{K_0^2 - K_3^2 - m^2} \cdot \frac{1}{2} (1 - i \gamma^1 \gamma^2 \text{sign}(eB))$$

projector

$$\begin{array}{l} 3+1 \longrightarrow 1+1 \\ 2+1 \longrightarrow 0+1 \end{array}$$

2

Dynamics underlying new plateaus
with $\nu=0$, $\nu=\pm 1$, $\nu=\pm 4$ observed
in graphene:

Y. Zhang et al., PRL 96 (2006) 136806;
Z. Jiang et al., PRL 99 (2007) 106802

"Old" plateaus:

$$\nu_{xy} = \frac{e^2}{h} \nu, \quad \nu = \pm 4(n + \frac{1}{2}), \quad n=0, 1, \dots$$

Experiment: K. Novoselov et al., Nature 438 (2005) 197,
Y. Zhang et al., Nature 438 (2005) 201

Theory: Y. Zheng and T. Ando, PRB 65 (2002) 245420,
V. Gusynin, S. Shcharikov, PRL 95 (2005) 146801;
N. Peres, F. Guinea, A. Castro Neto, PRB 73 (2006) ⁽¹²⁵⁴¹¹⁾

$$E_n = \pm \sqrt{2n\hbar v_F^2 |eB|/c} \approx 424 \sqrt{n} \sqrt{|B/T|} \text{ K}$$

$n=0, 1, 2, \dots$ $v_F \approx 10^6 \text{ m/s}$

LLL with $n=0$, $E_0=0$, is special

Nonrelativistic Dynamics in Magnetic Field

$$E_n \approx \frac{n \hbar \omega_F^2 |eB|}{c \cdot mc^2} \equiv n L(B) \cdot L(B)/mc^2,$$

$$L(B) \equiv \sqrt{\hbar \omega_F^2 |eB|} / c \approx 300 \sqrt{B[\text{T}]} \text{ K}$$

$$mc^2 \approx 0.5 \text{ MeV} \sim 10^{10} \text{ K}$$

$L(B)/mc^2 \ll 1$ for realistic
values of $B \lesssim 50 \text{ T}$

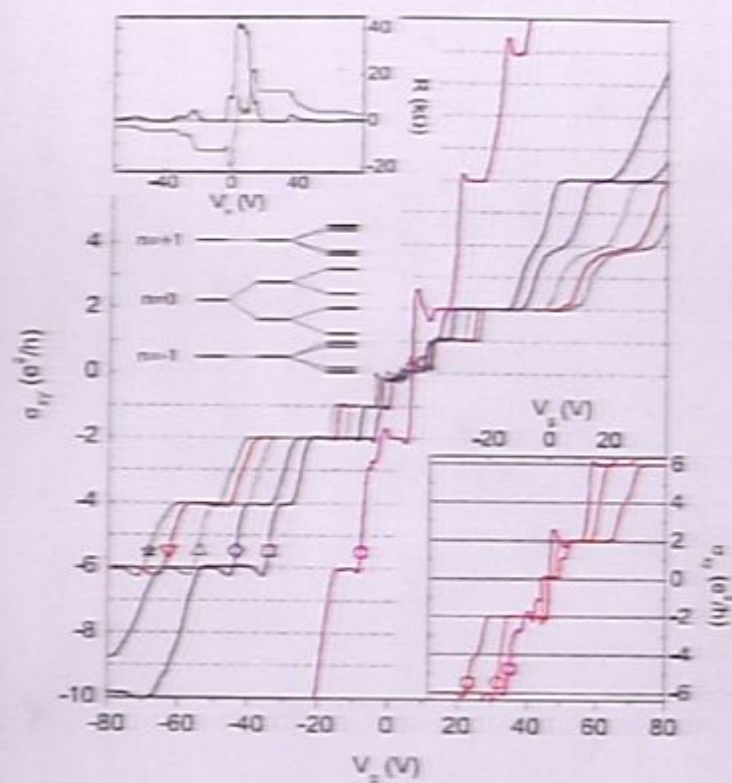


FIG 2. (color online) σ_{xx} as a function of V_g at different magnetic fields: 9 T (circle), 25 T (square), 30 T (diamond), 37 T (up triangle), 42 T (down triangle), and 45 T (star). All the data sets are taken at $T = 1.4$ K, except for the $B = 9$ T curve, which is taken at $T = 30$ mK. Left upper inset: R_L and R_R for the same device measured at $B = 25$ T. Left lower inset: a schematic drawing of the LLs in low (left) and high (right) magnetic field. Right inset: detailed σ_{xx} data near the Dirac point for $B = 9$ T (circle), 11.5 T (pentagon) and 17.5 T (hexagon) at $T = 30$ mK.

$$D = 4\left(n + \frac{1}{2}\right)$$

+2, +6, +10, ...

↓ NT Relevant direction

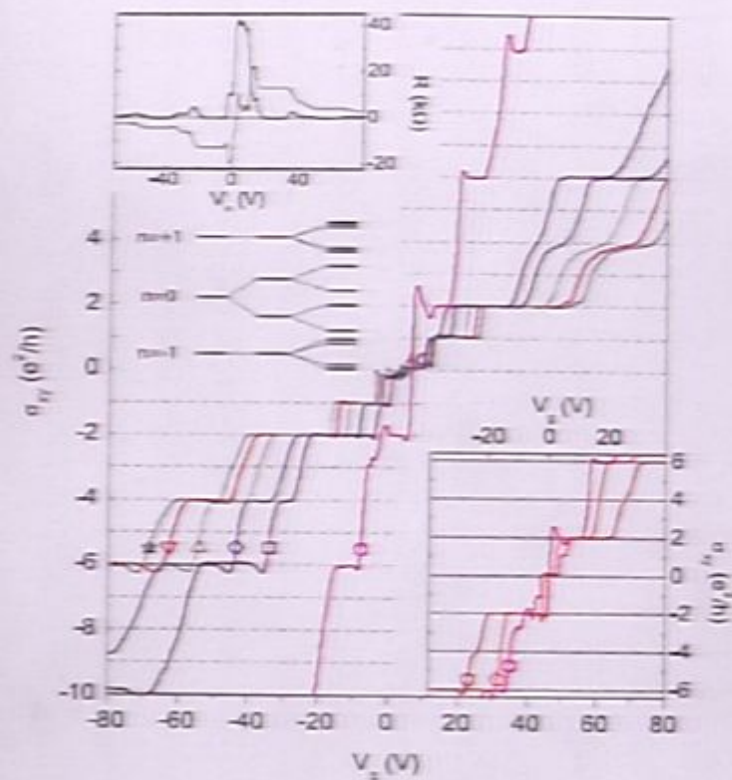


FIG 2. (color online) σ_{xx} as a function of V_g at different magnetic fields: 9 T (circle), 25 T (square), 30 T (diamond), 37 T (up triangle), 42 T (down triangle), and 45 T (star). All the data sets are taken at $T = 1.4$ K, except for the $B = 9$ T curve, which is taken at $T = 30$ mK. Left upper inset: R_L and R_T for the same device measured at $B = 25$ T. Left lower inset: a schematic drawing of the LLs in low (left) and high (right) magnetic field. Right inset: detailed σ_{xx} data near the Dirac point for $B = 9$ T (circle), 11.5 T (pentagon) and 17.5 T (hexagon) at $T = 30$ mK.

Model: Hamiltonian

$$H = H_0 + H_C - \mu_0 \psi_S^\dagger \psi_S + \mu_B B \psi_S^\dagger \sigma^3 \psi_S,$$

$\mu_B = e \hbar / 2mc$, $g_L \approx 2$, ($e > 0$); $B \equiv |\vec{B}|$

$$H_0 = \int_F d^2 \vec{r} \psi_S^\dagger (\gamma^1 \overleftrightarrow{\pi}_x + \gamma^2 \overleftrightarrow{\pi}_y) \psi_S,$$

$$\vec{r} = (x, y), \quad \overleftrightarrow{\pi} = (\overleftrightarrow{\pi}_x, \overleftrightarrow{\pi}_y) = -i \hbar \vec{\nabla} + e \vec{A} / c,$$

$v_F \approx 10^6$ m/s, $\psi_S = (\psi_{KAS}, \psi_{KBS}, \psi_{K'BS}, \psi_{K'AS})$,

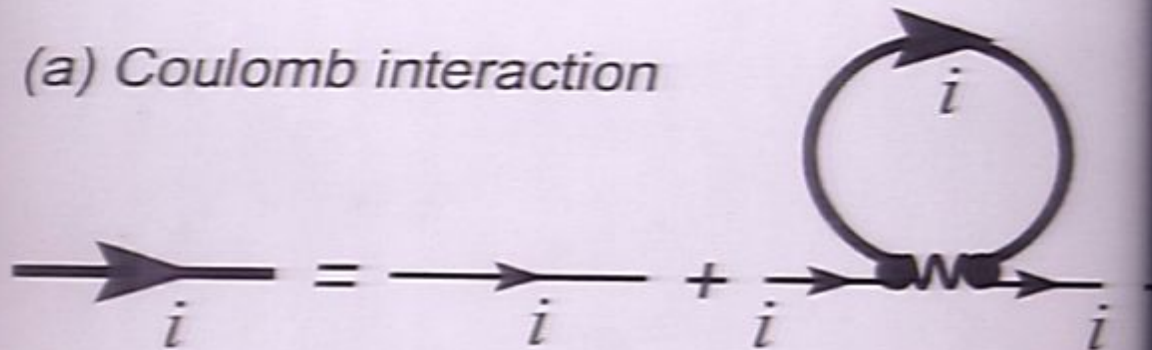
$\gamma^\nu = (\gamma^0, \gamma^1, \gamma^2) = \tilde{T}_{KK'}^3 \otimes (\tilde{T}^3, i\tilde{T}^2, -i\tilde{T}^1)_{AB}$,

$\overline{\psi}_S = \psi_S^\dagger \gamma^0$; \vec{A} corresponds to B_z .

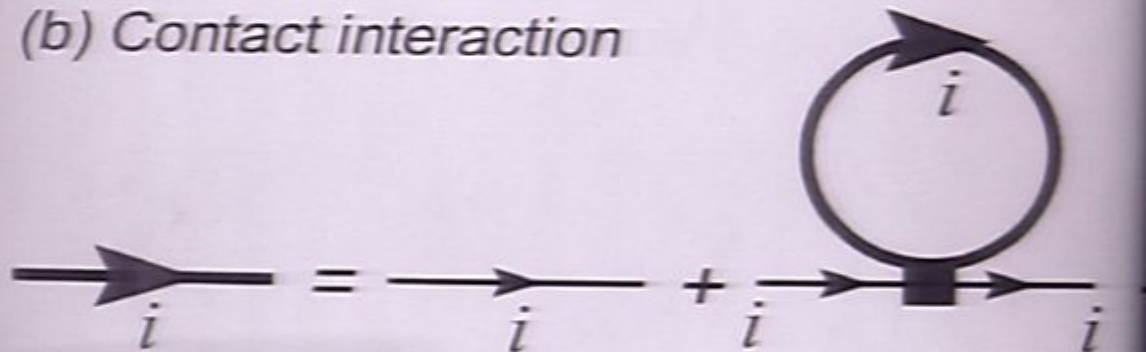
$$H_C = \frac{1}{2} \int d^2 \vec{r} d^2 \vec{r}' \psi_S^\dagger(\vec{r}) \psi_S(\vec{r}') \psi_S^\dagger(\vec{r}) \psi_S(\vec{r}') \psi_S^\dagger(\vec{r}) \psi_S(\vec{r}')$$

H_0 : Lorentz symmetry in 2+1 dimensions, with v_F playing the role of light velocity

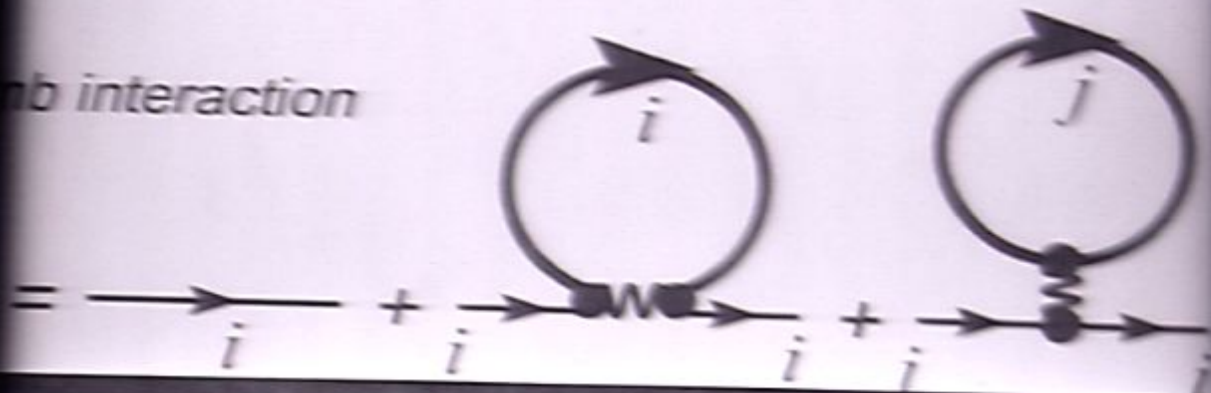
(a) Coulomb interaction



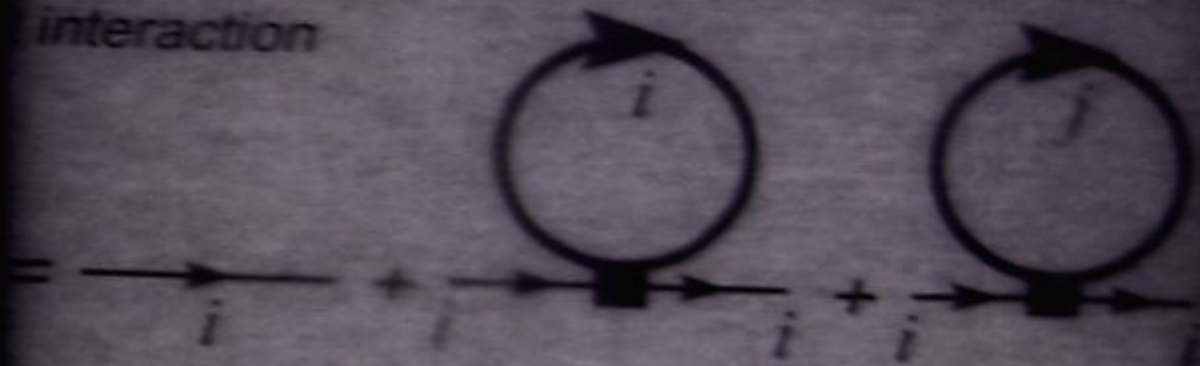
(b) Contact interaction



mb interaction



interaction



Model: Gap Equation

$G^-(u, u')$ - propagator of Dirac quasiparticles;
 $u \equiv (u_0, \vec{r})$, $u_0 \equiv t$.

Hartree-Fock (mean field) approximation:

$$G^-(u, u') = S^-(u, u') + i\hbar \gamma^0 G^-(u, u') \gamma^0 S(t-t') U_c(\vec{r}=\vec{r}') - i\hbar \gamma^0 \text{tr} [\gamma^0 G^-(u, u')] S(t-t') U_c(\vec{r}=\vec{r}') \uparrow$$

direct interactions

exchange interactions

$$i S^-(u, u') = [(i\hbar \partial_t + \mu_0 - \mu_B B \sigma^z) \gamma^0 - \vec{v}_F \vec{\sigma} \cdot \vec{\nabla}] S^-(u, u')$$

- bare inverse quasiparticle propagator

Approximation: $U_c(\vec{r}) \rightarrow G_{int} S^-(\vec{r})$

$$G^-(u, u') = S^-(u, u') + i\hbar G_{int} \gamma^0 G^-(u, u') \gamma^0 S^-(u, u') - i\hbar G_{int} \gamma^0 \text{tr} [\gamma^0 G^-(u, u')] S^-(u, u')$$

$$\Lambda \sim \lambda(B) \equiv \sqrt{\hbar |e B_{||}| / \hbar k}, \quad \lambda \equiv G_{int} \sqrt{\frac{v_F^2 + \mu^2}{\hbar v_F}}$$

London scale

dimensionless coupling constant

Hartree-Fock (mean field) approximation.

$$G^{-1}(u, u') = S^{-1}(u, u') + i\hbar \gamma^0 G(u, u') \gamma^0 \delta(t-t') U_c(\vec{r} - \vec{r}') - i\hbar \gamma^0 \text{tr} [\gamma^0 G(u, u')] \delta(t-t') U_c(\vec{r} - \vec{r}')$$

direct interactions exchange interactions

$$i S^{-1}(u, u') = [(i\hbar \partial_t + \mu_0 - \mu_B B \sigma^3) \gamma^0 - \gamma^i \partial_i \gamma^j] S^3(u, u')$$

- bare inverse quasiparticle propagator

Approximation: $U_c(\vec{r}) \rightarrow G_{int} S^3(\vec{r})$

$$G^{-1}(u, u') = S^{-1}(u, u') + i\hbar G_{int} \gamma^0 G(u, u') \gamma^0 \delta^3(u-u') - i\hbar G_{int} \gamma^0 \text{tr} [\gamma^0 G(u, u')] \delta^3(u-u')$$

$\Lambda \sim L(B) \equiv \sqrt{\hbar |eB|} / \hbar v_F$, $\lambda \equiv G_{int} \sqrt{\frac{2\pi \hbar^2 v_F^2}{\mu_0 \hbar v_F}}$

Landau scale dimensionless coupling constant

$$G^{-1}(u, u') = S^{-1}(u, u') + i\hbar \gamma^0 G(u, u') \gamma^0 \delta(t-t') U_c(\vec{r}-\vec{r}') -$$

$$- i\hbar \gamma^0 \text{tr} [\gamma^0 G(u, u')] \delta(t-t') U_c(\vec{r}-\vec{r}')$$

direct interactions exchange interactions

$$i S^{-1}(u, u') = [(i\hbar \partial_t + \mu_0 - \mu_B B \sigma^3) \gamma^0 - \gamma^i \vec{v}_F \cdot \vec{\sigma}] S^3(u, u')$$

- bare inverse quasiparticle propagator

Approximation: $U_c(\vec{r}) \rightarrow G_{\text{int}} \delta^3(\vec{r})$

$$G^{-1}(u, u') = S^{-1}(u, u') + i\hbar G_{\text{int}} \gamma^0 G(u, u') \gamma^0 \delta^3(u-u') -$$

$$- i\hbar G_{\text{int}} \gamma^0 \text{tr} [\gamma^0 G(u, u')] \delta^3(u-u')$$

$$\Lambda \sim L(B) \equiv \sqrt{\hbar |eB_{||}| \frac{v_F^2}{c}}, \quad \lambda \equiv G_{\text{int}} N \frac{v_F^2}{(4\pi \hbar v_F)}$$

Landau scale

dimensionless coupling constant

passes the $U(4)$ symmetry with 16 generators:

$$\frac{\sigma^a}{2} \otimes I_4, \frac{\sigma^a}{2i} \otimes \gamma^3, \frac{\sigma^a}{2} \otimes \gamma^5, \frac{\sigma^a}{2} \otimes \gamma^3 \gamma^5,$$

where I_4 - 4x4 Dirac unit matrix, σ^a - four Pauli matrices (σ^0 is 2x2 unit matrix),

$$\gamma^3 = i \begin{pmatrix} 0 & I \\ I & 0 \end{pmatrix}, \gamma^5 = i \begin{pmatrix} 0 & I \\ -I & 0 \end{pmatrix}, \text{ and } \gamma^3 \gamma^5 = \begin{pmatrix} I & 0 \\ 0 & -I \end{pmatrix} - \text{pseudospin matrix}$$

Zeeman term $M_B \psi_s^\dagger \sigma^3 \psi_s$ breaks $U(4)$ down to $U(2)_+ \times U(2)_-$ with 8 generators $I_4 \otimes P_s, \gamma^5 \otimes P_s, -i\gamma^3 \otimes P_s,$ and $\gamma^3 \gamma^5 \otimes P_s$; $s = \pm, P_\pm = (1 \pm \sigma_3)/2$ are projectors on spin up and down states

Order Parameters

Goal: searching for solutions of gap equation with spontaneously broken and unbroken $SU(2)_s$, $U(1)_s$, $S=\pm$

Two scenarios for QH effect

a) Quantum Hall Ferromagnetism (QHF)

(K. Nomura, A. MacDonald, PRL 96 (2006) 256602;
M. Goerdig, R. Moessner, B. Douçot, PRB 74 (2006) 161407;
J. Alicea and M.P.A. Fisher, PRB 74 (2006) 075422;)

Order parameters: pseudospin densities

$\langle \Psi^\dagger \gamma^3 \gamma^5 P_s \Psi \rangle \neq 0 \Rightarrow SU(2)_s \rightarrow U(1)_s$
with the generator $\gamma^3 \gamma^5 \otimes P_s$, $P_s = \frac{L \pm G^3}{2}$

$\tilde{\mu}_s$ are corresponding chemical potentials. Triplet order parameters

Scenario is based on conventional ferromagnetism

Goal: searching for solutions of gap equation with spontaneously broken and unbroken $SU(2)_s$, $U(1)_s$, $S=\pm$

Two scenarios for QH effect

a) Quantum Hall Ferromagnetism (QHF)

(K. Nomura, A. MacDonald, PRL 96 (2006) 256602;
M. Goerbig, R. Moessner, B. Douçot, PRB 74 (2006) 161407;
J. Alicea and M.P.A. Fisher, PRB 74 (2006) 075422;)

Order parameters: pseudospin densities
 $\langle \psi^\dagger \gamma^3 \gamma^5 P_s \psi \rangle \neq 0 \Rightarrow SU(2)_s \rightarrow U(1)_s$
with the generator $\gamma^3 \gamma^5 \otimes P_s$, $P_\pm = \frac{L \pm \sigma^3}{2}$
 $\tilde{\mu}_s$ are corresponding chemical potentials. Triplet order parameters
Scenario is based on conventional ferromagnetism

7
b) Magnetic Catalysis (MC)

(V. Gusynin, V. Miransky, S. Shcharapov, I. Shorkov, PRL 74 (2006) 195429; I. Herbut, PRL 97 (2006) 146401; J. Fuchs, P. Lederer, PRL 98 (2007) 016803)

Order parameters: Dirac mass terms
 $\langle \bar{\psi} \beta_5 \psi \rangle \equiv \langle \psi^\dagger \gamma^0 \beta_5 \psi \rangle \neq 0 \implies$
 $SU(2)_5 \rightarrow U(1)_5$

$\tilde{\Delta}_5$ are corresponding Dirac masses (gaps).

Triplet order parameters.

Scenario is based on relativistic 2+1 dimensional dynamics in magnetic field

V. Gusynin, V. Miransky, I. Shorkov, PRL 73 (1994) 3499

In graphite:

D. Khveshchenko, PRL 87 (2001) 206401;

E. Gorbar, V. Gusynin, V. Miransky, I. Shorkov, PRB 66 (2002) 045108

8

Latest developments: QHF and MC sets of order parameters necessarily coexist, which implies that they have the same dynamical origin.

E. Gorbar, V. Gusynin, V. Miransky, arxiv: 0710.3527 [cond-mat]

E. Gorbar, V. Gusynin, V. Miransky, I. Shovkovy, (to appear)

General form of inverse quasiparticle propagator:

$$iG_s^{-1}(2l, 2l') = \left[(i\hbar\partial_t + \mu_s + \tilde{\mu}_s \gamma^3 \gamma^5) - \gamma_F \vec{\sigma} \vec{\gamma} + \Delta_s \gamma^3 \gamma^5 - \tilde{\Delta}_s \right] S^3(2l - 2l')$$

One more surprise: Δ_s — $SU(2)_s$ singlet Dirac mass $\Rightarrow \langle \bar{\psi} \gamma^3 \gamma^5 \psi \rangle$. It is odd under time reversal

Δ_s in graphite with no magnetic field:

F. D. M. Haldane, PRL 61 (1988) 2015

Parity anomaly in $(2+1)$ dimensional QFT:

R. Jackiw;

A. Niemi, G. Semenoff

Latest developments: QHF and MC
sets of order parameters necessarily
coexist, which implies that they have
the same dynamical origin.

E. Gorbar, V. Gusynin, V. Miransky, arxiv:
0710.3527 [cond-mat]

E. Gorbar, V. Gusynin, V. Miransky, I. Shonkova,
(to appear)

General form of inverse quoniparticle propagator:
$$iG_S^{-1}(u, u') = \left[(i\hbar\partial_t + \mu_S + \tilde{\mu}_S \gamma^3 \gamma^5) - \gamma_F \vec{u} \vec{\gamma} + \Delta_S \gamma^3 \gamma^5 - \tilde{\Delta}_S \right] S^3(u - u')$$

One more surprise: Δ_S — $SU(2)_S$ singlet Dirac
mass $\Rightarrow \langle \bar{\psi} \gamma^3 \gamma^5 \psi \rangle$. It is odd under time
reversal

Δ_S in graphite with no magnetic field:

F. D. M. Haldane, PRL 61 (1988) 2015

Parity anomaly in $(2+1)$
dimensional QFT:

R. Jackiw;

A. Niemi, G. Semenoff

8
Latest developments: QHF and MC sets of order parameters necessarily coexist, which implies that they have the same dynamical origin.

E. Gorbar, V. Gusynin, V. Miransky, arxiv: 0710.3527 [cond-mat]

E. Gorbar, V. Gusynin, V. Miransky, I. Shovkova, (to appear)

General form of inverse quoniparticle propagator:
$$iG_S^{-1}(x, x') = [(i\hbar\partial_t + \mu_S + \tilde{\mu}_S \gamma^3 \gamma^5) - \gamma_F \vec{\sigma} \vec{\gamma} + \Delta_S \gamma^3 \gamma^5 - \tilde{\Delta}_S] S^3(x-x')$$

One more surprise: Δ_S - $SU(2)_S$ singlet Dirac mass $\Rightarrow \langle \bar{\psi} \gamma^3 \gamma^5 \psi \rangle$. It is odd under time reversal

Δ_S in graphite with no magnetic field:

F. D. M. Haldane, PRL 61 (1988) 2015

Parity anomaly in $(2+1)$ dimensional QFT:

R. Jackiw;

A. Niemi, G. Semenoff

8
Latest developments: QHF and MC sets of order parameters necessarily coexist, which implies that they have the same dynamical origin.

E. Gorbar, V. Gusynin, V. Miransky, arxiv: 0710.3527 [cond-mat]

E. Gorbar, V. Gusynin, V. Miransky, I. Shovkova, (to appear)

General form of inverse quasiparticle propagator:
$$iG_S^{-1}(z, z') = [(i\hbar\partial_t + \mu_S + \tilde{\mu}_S \gamma^3 \gamma^5) - \gamma^0 \vec{\gamma} \vec{\gamma} + \Delta_S \gamma^3 \gamma^5 - \tilde{\Delta}_S] S^3(z - z')$$

One more surprise: Δ_S - s.u(2)_S singlet Dirac mass $\Rightarrow \langle \bar{\psi} \gamma^3 \gamma^5 \psi \rangle$. It is odd under time reversal

Δ_S in graphite with no magnetic field:

F. D. M. Haldane, PRL 61 (1988) 2015

Parity anomaly in (2+1) dimensional QFT:

R. Jackiw,

A. Niemi, G. Semenoff

Dispersion Relations

$$i\tilde{G}_s^{-1}(\omega, \vec{v}) = [(i\hbar\partial_t + \mu_s + \tilde{\mu}_s \gamma^3 \gamma^5) \gamma^0 - \vec{\sigma}_F \vec{\gamma} \vec{\gamma} + \Delta_s \gamma^3 \gamma^5 - \tilde{\Delta}_s] \mathcal{S}^3(\omega - \vec{v})$$

LLL

$$\omega_s^{(0)} = -\mu_s + \mathcal{G} [\tilde{\mu}_s \text{sign}(eB_z) + \tilde{\Delta}_s] + \Delta_s \text{sign}(eB_z)$$

Higher LLs ($|m| \geq 1$)

Dispersion Relations

$$i\tilde{\sigma}_s^{-1}(\omega, \omega') = [(i\hbar\partial_t + \mu_s + \tilde{\mu}_s \gamma^3 \gamma^5) \gamma^0 - \sigma_F \vec{\gamma} \cdot \vec{\omega} + \Delta_s \gamma^3 \gamma^5 - \tilde{\Delta}_s] \delta^3(\omega - \omega')$$

LLL

$$\omega_s^{(0)} = -\mu_s + \sigma [\tilde{\mu}_s \text{sign}(eB_L) + \tilde{\Delta}_s] + \Delta_s \text{sign}(eB_L)$$

Higher LLs ($m \geq 1$)

$$\omega_{ms}^{(0)} = -\mu_s + \sigma \tilde{\mu}_s + \text{sign}(m) \sqrt{2\hbar |neB_L| \sigma_F^2 / c + (\tilde{\Delta}_s + \sigma \Delta_s)^2}$$

Conclusion

1. It seems QHF and MC scenarios are two sides of the same coin.
2. Generating dynamical Dirac masses in tabletop experiment.
3. Consequences for dynamics of edge states.
4. Potential consequences for (pseudo-)NG excitations.
5. "Convergence" of QHF and MC scenarios is a good sign for theory.

Conclusion

1. It seems QHF and MC scenarios are two sides of the same coin.
2. Generating dynamical Dirac masses in tabletop experiment.
3. Consequences for dynamics of edge states.
4. Potential consequences for (pseudo-)NG excitations.
5. "Convergence" of QHF and MC scenarios is a good sign for theory.

1. It seems QHF and MC scenarios are two sides of the same coin.
2. Generating dynamical Dirac masses in tabletop experiment.
3. Consequences for dynamics of edge states.
4. Potential consequences for (pseudo-)WG excitations.
5. "Convergence" of QHF and MC scenarios is a good sign for theory.

or tabletop experiment.

3. Consequences for dynamics of edge states.
4. Potential consequences for (pseudo-)Weyl excitations.
5. "Convergence" of QHF and MC scenarios is a good sign for theory.